Theoretical prediction of fast 3D AC electro-osmotic pumps

Martin Z. Bazant* and Yuxing Ben

Received 7th June 2006, Accepted 8th August 2006
First published as an Advance Article on the web 4th September 2006
DOI: 10.1039/b608092h

AC electro-osmotic (ACEO) pumps in microfluidics currently involve planar electrode arrays, but recent work on the underlying phenomenon of induced-charge electro-osmosis (ICEO) suggests that three-dimensional (3D) geometries may be exploited to achieve faster flows. In this paper, we present some new design principles for periodic 3D ACEO pumps, such as the "fluid conveyor belt" of ICEO flow over a stepped electrode array. Numerical simulations of these designs (using the standard low-voltage model) predict flow rates almost twenty times faster than existing planar ACEO pumps, for the same applied voltage and minimum feature size. These pumps may enable new portable or implantable lab-on-a-chip devices, since rather fast (mm s^{-1}), tuneable flows should be attainable with battery voltages (<10 V).

Introduction

The ability to manipulate fluids in microchannels with ease and precision is central to the lab-on-a-chip concept.[1] This goal has been achieved for a range of applications by networks of peristaltic pumps and valves[2] fabricated by soft lithography.[3] Traditional pressure-driven flows, however, do not scale well with miniaturization and often require complicated off-chip plumbing (which limits portability), so a variety of other pumping techniques have also been explored.[4]

An attractive alternative is electro-osmosis,[5] the effective slip of a liquid electrolyte past a solid surface in response to an applied electric field, since it does not involve any moving parts, is unaffected by miniaturization, and integrates well with standard microelectronics and fabrication methods. The well established technique of (capillary) electro-osmosis involves a DC electric field applied down a microchannel made of insulating material to generate a plug flow. The electric field acts on the equilibrium surface charge in the diffuse-part of the double layer, and the resulting electro-osmotic flow is linear in the applied field.

Various methods have been described to alter the surface charge in linear electro-osmosis to allow some degree of local flow control. In the early 1990s, "field-effect electro-osmosis" was proposed to control capillary electro-osmosis by applying large (kV) voltages at secondary electrodes just outside the channel surface, to alter the equilibrium surface charge (or zeta potential) driving steady flow at the insulating channel wall.[6] A similar design with a lower "gate voltage" (>10 V) has been called a "flow-FET" by analogy to the field-effect transistor in micro-electronics (where a gate voltage controls the flow of electrons, instead of a liquid).[7]

Capillary electro-osmosis, with or without field-effect flow control, has some serious drawbacks for certain microfluidic applications: (i) Since the electric field is applied down the channel, a large voltage is required, *e.g.* 100 V across a 1 cm microfluidic chip to produce 100 V cm^{-1} fields. (ii) Since the electro-osmosis is linear in the applied field, a direct current must be sustained through Faradaic electrochemical reactions at the electrodes generating the field, which can produce gas bubbles, electrode degradation/dissolution, hydrodynamic instability, and sample contamination. (iii) The typical fluid velocity is fairly small ($u \sim 100$ μm s^{-1} for $E \sim 100$ V cm^{-1}) and only increases linearly with the voltage. In many lab-on-a-chip applications, it would be preferable to drive flows with low-voltage alternating currents, while also increasing the flow rate for the same applied field.

These drawbacks do not apply to nonlinear electro-osmotic flows (varying nonlinearly with the applied voltage), which have been used to drive flows over two-dimensional, co-planar electrodes applying alternating voltages. Ramos *et al.* reported the first experimental observation of quadratically nonlinear electro-osmotic flow ($u \sim V^2$) sucking in fluid between a pair of electrodes on the wall of a microchannel, and they developed a theory based on capacitive charging of the diffuse layer.[8] The peak velocity occurs at a particular AC frequency (the inverse "RC time" of double-layer charging[9]) and decays above and below this resonance, so they called the effect "AC electro-osmosis" (ACEO).

Soon afterwards, Ajdari predicted that ACEO could be used to pump fluids over a periodic parallel-stripe electrode array by taking advantage of various broken symmetries.[10] Specifically, he suggested either modifying the surface capacitance (*via* a partial coating on each electrode) or simply modulating the surface height, but neither of these suggestions has ever pursued. Instead, Brown *et al.* proposed breaking symmetry with pairs of co-planar flat electrodes of different widths and spacing in a periodic array, and they fabricated the first ACEO pumps in this way, followed closely by several other groups.[11] Recently, Cahill *et al.* have also suggested using a traveling wave voltage (as opposed to a standing wave) to drive ACEO flow over symmetric planar electrode arrays and have demonstrated radial pumping over interdigitated spiral electrodes.[12]

Institute of Soldier Nanotechnologies and Department of Mathematics, Massachusetts Institute of Technology, Cambridge, MA 02139-4307, USA. E-mail: bazant@mit.edu; Fax: +1 (617) 253-8911; Tel: +1 (617) 253-1713

The two-dimensional (flat, co-planar) electrode array is the only geometry that has been pursued in designing ACEO pumps, and little improvement in the flow rate has been achieved since the initial work. The state of the art is represented by the design of Brown *et al.*,[11] characterized in the recent experiments by Studer *et al.*,[13] which we use as a baseline case for comparision with our new designs below. ACEO pumps operate at much lower power (<10 mW) and lower voltage (<10 V) than pumps based on linear capillary electro-osmosis, so they hold great promise for portable or implantable microfluidics. Planar ACEO pumps are still relatively weak for long-range pumping ($u \sim 100$ μm s^{-1}), but the full set of possible designs has hardly been explored.

In this paper, we predict that certain, three-dimensional (3D) geometries can dramatically increase flow rates, compared to planar ACEO pumps, at the same applied voltage and minimum feature size. We are motivated by the recent work of Bazant and Squires on "induced-charge electro-osmosis" (ICEO),[14] which unifies ACEO with other nonlinear electro-osmotic flows around polarizable colloids[15] and microstructures.[16] In particular, we build on their suggestion of shaping ICEO flows in three dimensions with metal structures protruding into a microchannel.

The paper is organized as follows. We begin by describing design principles for 3D ACEO pumps, such as the "fluid conveyor belt" of ICEO flow over stepped electrodes. We then perform numerical simulations (using the standard low-voltage model[16]) of a few stepped ACEO pumps and predict that they are almost twenty times faster than existing planar ACEO pumps[11,13] at the same applied voltage and minimum feature size. We conclude by briefly discussing implications for microfluidics.

General 3D design principles

We consider standard microfluidic devices where metal structures and electrodes are patterned onto a flat substrate, typically glass or silicon, to form an electrokinetic "pump".[10–14] The fluid is pumped down a microchannel, *e.g.* which may be formed by a molded-polymer cap fabricated by soft lithography. In such channels designed for biological or chemical analysis, the upper surface and side walls may have embedded sensors. In channels for long-range pumping, pressure generation, or electrokinetic injection, the upper surface may consist of a similar electrokinetic pump (on an upside-down substrate) with the channel formed by sandwiching a spacer layer in between. Hereafter, we focus on the design of the pump geometry, as fabricated on a flat substrate.

The "fluid conveyor belt"

Whether in metallic colloids or in microfluidic devices, ICEO flows involve non-uniform polarization of the double layer, and thus a non-uniform electro-osmotic slip distribution, in response to an applied electric field.[14] In symmetric situations, the contributions of opposing slip cancel to produce no net electrophoretic motion or long-range fluid pumping, respectively, for a metal colloidal sphere in a uniform DC or AC electric field[15] or a symmetric pair of electrodes applying an AC voltage.[8] As first suggested by Ajdari,[10] net pumping by ACEO at electrode arrays can only be achieved by breaking spatial symmetry in each period. Traveling-wave electro-osmosis similarly takes advantage of temporal symmetry breaking. Broken symmetry is also required for induced-charge electrophoresis of polarizable (conducting or dielectric) colloids.[14]

For this reason, it would seem that ICEO is inherently inefficient for fluid pumping over a surface (or electrophoretic motion), since the surface-averaged slip will always be much smaller than the maximum slip, due to the cancellation of opposing velocities. Certainly, this is the case with existing planar ACEO pumps,[11–13] where ~mm s^{-1} maximum velocities yield only ~100 μm s^{-1} surface averaged slip velocities. This thinking, however, only applies to flat surfaces, where the opposing slip regions are aligned in maximal competition.

In three dimensions, it is possible to design surfaces of nonuniform slip where essentially every region of the surface contributes to fluid pumping in a single direction. The simple principle, which applies to any situation of nonuniform slip (not just ICEO), is to create a "fluid conveyor belt" by raising regions pumping in the desired direction and recessing regions of reverse slip, as shown in Fig. 1. For an appropriate choice of the step height, the vortices driven by reverse slip on the recessed surfaces will recirculate near the level of the raised surfaces, thus providing "rollers" for the fluid conveyor belt. It is intuitively obvious that these vortices will enhance the pumping flow substantially, even compared to having no-slip surfaces in place of the reverse-slip regions.

There are several ways to use electro-osmotic flows to create a fluid conveyor belt in a microfluidic device. The conceptually simplest case is shown in Fig. 2(a), where a background electric field (supplied by more distant, unscreened electrodes) passes over a surface with raised and lowered steps of alternating diffuse-layer charge (or zeta potential) to create the slip profile

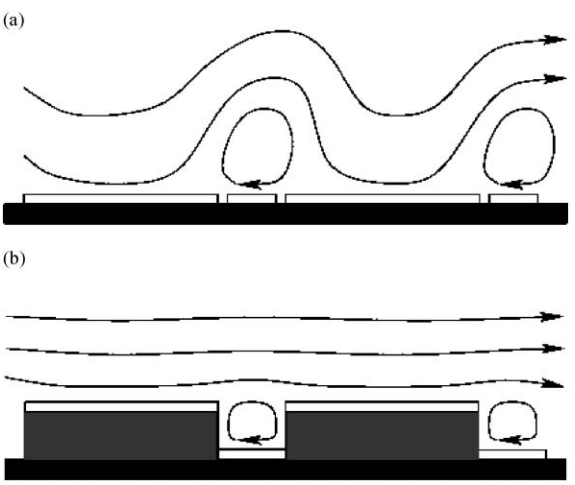

Fig. 1 The Fluid Conveyor Belt Principle. (a) A sketch of the flow above a flat surface which contains regions of fluid slip in opposite directions. The counter-rotating vortices above the smaller/slower regions inhibit the long-range pumping flow driven of larger/faster regions. (b) A sketch of the much faster flow above a non-planar surface with raised pumping regions where the counter-rotating vortices are recessed to form the "rollers" of a "fluid conveyor belt".

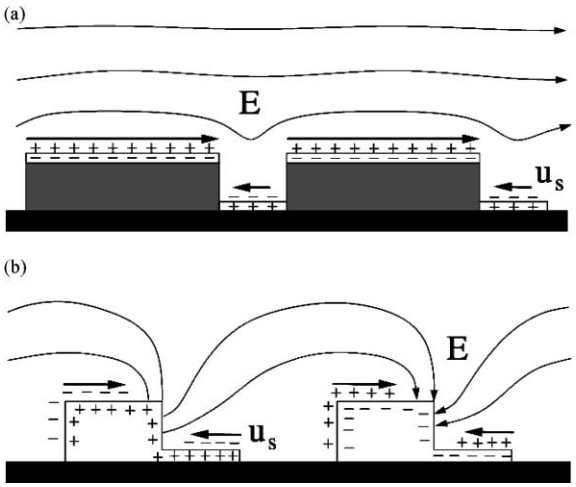

Fig. 2 Physical mechanisms for the electrical generation of a fluid conveyor belt. ICEO slip (thick arrows, u_s) producing a flow similar to Fig. 1(b) is driven by the electric field (solid curves, E) acting on induced diffuse-layer charge (+,−) on electrodes (polarized as +,−) in a periodic array. (a) Fixed-potential ICEO driven by a DC or AC background electric field (applied at more distant, unscreened electrodes, not shown) over fully screened pumping electrodes. (b) ACEO at the resonant frequency, where each electrode is partially screened at its edges, while supplying the electric field from its center.

and flow in Fig. 1(b). With a steady DC field, this flow can be produced by standard linear electro-osmosis with non-polarizable surfaces of fixed equilibrium charge (*e.g.* due to different coatings on the raised and lowered surfaces). However, linear electro-osmotic pumping is more easily achieved with a homogenous surface of maximal equilibrium zeta potential.

Instead, the purpose of the fluid conveyor belt concept is to efficiently rectify non-uniform ICEO flows at polarizable surfaces in AC fields. For example, if the stepped surfaces are electrodes, it is possible to achieve the diffuse-charge distributions in Fig. 2(a) through capacitive coupling by appropriately controlling their voltages in an AC (or DC) background electric field. The resulting fixed-potential ICEO flows drive a fluid conveyor belt pumping in one direction. Perhaps the simplest electrical connections would involve grounding the raised electrodes to one background electrode (supplying the electric field) and the lowered electrodes to the other background electrode. The pump would operate in the range of AC frequencies where the stepped electrodes become fully screened by diffuse charge, while the background electrodes remain unscreened.[14] (These "RC" charging times[9] are discussed below.)

The fluid conveyor belt concept can also be applied to ACEO at partially-screened electrodes, which also supply the electric field, near the resonant RC frequency. In this case, the electric field is larger than in fixed-potential ICEO designs, for the same applied voltage, since there is no need to separate the background and pumping electrodes. ACEO flows at planar electrode arrays are generally strongest near the electrode edges and directed toward the electrode centers.[8] It is natural therefore to raise the portion of the each electrode pumping in a desired direction (or lower the other portions) to create a fluid conveyor belt. As shown in Fig. 2(b), the charge and slip profiles are more complicated than with fixed-potential ICEO at fully screened electrodes, but the conveyor-belt principle leading to efficient pumping in one direction is the same. Below we will analyze such 3D ACEO pumps with numerical simulations, which predict that they are almost twenty times faster than planar ACEO pumps under similar conditions.

Geometrical field amplification

There is another, secondary, advantage of 3D electrode designs: enhancement of the electric field by geometrical confinement. A simple, unexpected effect of this type in planar ACEO has been noted recently by Olesen *et al.*[17] They predicted that the average ACEO velocity past a planar asymmetric electrode array is enhanced, by up to a factor of two, when the channel height is reduced to the scale of the spatial period. The reason is that electric field lines are confined by the opposite wall, thus increasing the typical field strengths near the electrodes driving ACEO flow.

With 3D electrode structures, the electric field can be manipulated to a greater degree, *e.g.* by introducing field singularities at corners and confined local "channels" for the electric field. In the regions of greatest slip, the electrode surface is fully screened and acts like an insulator. In a planar geometry as in Fig. 1(a), the electric field is bounded, but at a protruding corner it becomes singular. For example, in Fig. 2(a), the raised electrode makes an angle of $3\pi/2$ with the side wall, so the electric field has an insulating-corner singularity of $E \sim r^{-1/3}$. In Fig. 2(b), the same singularity occurs at the outer corner of the raised electrode surface, which amplifies the pumping flow. The geometrical confinement of the electric field emanating from the recessed surfaces and side walls enhances its strength before it fans out over the raised electrodes.

Three-dimensional geometry can also affect the double-layer charging process and thus the frequency spectrum of ACEO flow. For example, the edge of an electrode on a flat insulating surface has an initial field singularity, $E \sim r^{-1/2}$, which locally accelerates double-layer charging prior to complete screening. For a raised electrode with an insulating side wall, as in Fig. 2(a), the field singularity is enhanced, $E \sim r^{-2/3}$, so the charging will occur more quickly, thus shifting the decay of ACEO flow to higher frequencies. For a stepped electrode with conducting side walls as in Fig. 2(b), the initial singularity is weaker, $E \sim r^{-1/3}$, but after double-layer polarization the field remains singular, $E \sim r^{-1/3}$, as noted above.

Fast 3D ACEO pumps

When Ajdari first introduced ACEO pumps,[10] he noted that surface height modulation could provide the symmetry breaking needed to achieve pumping over a periodic array of electrodes, and he calculated the pumping velocity to first order in a small sinusoidal height perturbation. All subsequent theoretical and experimental work on ACEO, however, has focused on planar electrode arrays, where symmetry is broken instead by the spacings and sizes of the pair of electrodes in each period.[11–13] We will show that this is not the most effective means of symmetry breaking in ACEO. Non-planar electrode arrays, setting up a fluid conveyor belt with stepped

electrodes (with "large" perturbations in surface height) will make much more efficient pumps.

Numerical simulations

To theoretically compare different pump designs, we employ the same simulation method as in our previous work and refer the reader to the paper of Levitan *et al.* for details.[16] Briefly, since the geometries are complicated, we use a commercial finite-element package (FEMLAB) to solve the standard model equations for ICEO flows in weak electric fields with thin double layers.[8,10–16] We assume symmetry transverse to the flow direction and thus perform only two-dimensional simulations. We employ periodic boundary conditions in the pumping direction, so the simulation corresponds to a microfluidic loop with its floor covered by the electrode array, without any "external" hydrodynamic resistance in series. The ceiling of the channel is a no-slip surface at a distance much larger than the electrode and vortex sizes.

We first solve the electrochemical equivalent-circuit problem, where the electostatic potential satisfies Laplace's equation (for an Ohmic bulk resistance) with time-dependent boundary conditions for double-layer charging (for a thin surface capacitor). For this work, we model the double layer on each electrode as simply a linear capacitance, ignoring any frequency dispersion or nonlinearity. Once the electrochemical problem is solved, the Helmholtz–Smoluchowski formula gives the slip velocity driving a Stokes flow. We solve for the time-averaged flow profile, assuming linear response at the AC driving frequency.

We work with dimensionless variables appropriate for ACEO,[8–16] set by the minimum feature size L of the geometry, which is typically comparable to the electrode spacing. Time is scaled to the "RC time" for double-layer charging,[9] $\tau = \lambda L/D(1 + \delta)$, where λ is the Debye screening length, D is the electrolyte diffusivity, and δ is the ratio of the diffuse and compact layer (linear) capacitances. Fluid velocity is scaled to the typical ACEO speed, $U = \varepsilon V^2/\eta L(1 + \delta)$, where V is the applied voltage and ε and η are the permittivity and viscosity of the solvent, respectively.[8,10] This is the same scale as for ICEO flow around a non-electrode metal surface,[14–16] $U = \varepsilon LE^2/\eta(1 + \delta)$, where $E = V/L$ is the scale of the electric field.

In order to make a fair comparision between different pumps, we fix the applied voltage V and the minimum feature size L. The fabrication method by various lithographic methods usually sets the latter as the minimum width of the "footprint" of a single feature, such as a gap or step (viewed from above). The flow rate, Q, is obtained by integrating the horizontal velocity across a vertical line through the channel. For a channel height H, the flow rate has units of UH $= \varepsilon V^2 H/\eta(1 + \delta)L$ (volume of fluid per transverse length per time = area/time). A mean velocity in the channel is $u = Q/H$. In all of our simulations, we use $H/L = 20$, so we expect our results for the flow rate to apply to any "wide" channel with $H \gg L$, with appropriate scaling of the dimensionless variables.

Stepped electrode arrays

We begin by recalling the ACEO flow above a periodic array of symmetric, planar electrode pairs, which, of course, cannot act as a pump. The time-averaged fluid streamlines near the resonant frequency exhibit well-known counter-rotating vortices.[8–13] The maximum slip velocity arises at the edges and is directed toward the center of each electrode. These converging flows meet at a stagnation point at the center and recirculate into the bulk. If the channel has a finite height, the streamlines close to form a vortex pair over each electrode.

As explained above, to create a fluid conveyor belt pumping in one direction, say to the right, we can either lower the electrode regions slipping to the left or raise those slipping to the right. In both cases, the goal is to recess the left-slipping vortex so that it recirculates at the level of right-slipping surfaces to enhance (rather than inhibit) pumping to the right. Of course, changing the electrode geometry affects the electric field and induced double-layer charge, and thus the slip velocity distribution, but we expect that it will not be qualitatively different from the planar geometry, where fluid is sucked in from the edge of each electrode toward the central region, where it is ejected into the bulk. (This is analogous to ICEO flow around a metal particle or post of arbitrary shape in a uniform electric field, which sucks fluid in along the field axis and ejects it radially.[14–16])

As a first approximation, therefore, we can try to create a fluid conveyor belt by looking at the slip distribution over a planar electrode array and raising the regions slipping in the desired direction; the height difference should be roughly equal to the width of the recessed slipping region (say, half the width of the recessed electrode), since Stokes flow has no intrinsic length scale. This very simple design principle turns out to be remarkably effective, as we now demonstrate through several examples, where no additional optimization of the geometry has been done. First, in Fig. 3a, we consider raising the left half of each electrode in a symmetric array by one quarter of its width. As shown in Fig. 3b for $\omega = 1/\tau$, this successfully creates a fluid conveyor belt pumping from left to right, resembling the sketch in Fig. 1b. The electric field lines in phase with the AC forcing (real part of the complex amplitude), shown in Fig. 3c, also resemble the sketch in Fig. 2b, which indicates how the electrodes are polarized.

To test the efficiency of this 3D ACEO pump, we compare to simulations of the current state-of-the-art in planar ACEO pumps, introduced by Brown *et al.*[11] and characterized in the recent experiments of Studer *et al.*[13] In this planar design, symmetry is broken by using two different electrode widths and spacings as shown in Fig. 4a. The streamlines are shown in Fig. 4b for $\omega = 1/\tau$. The flow profile of the planar pump resembles the sketch in Fig. 1a, where long-range flow is achieved by tortuous streamlines, which must bypass reverse vortices. This is rather inefficient, and the surface-averaged slip velocity (which sets the flow rate in an effective Poiseuille flow for a channel with a nonuniform slip distribution[18]) is orders of magnitude smaller than the maximum slip velocity. We will show that a "lost order of magnitude" in flow rate can be recovered through the fluid conveyor belt design, which more efficiently harnesses the power of ACEO flow.

As shown in Fig. 5, the increase in flow rate is quite dramatic. Without any geometrical optimization, the stepped electrode array of Fig. 3 achieves a maximum flow rate of $Q_{max} = 27.4 \times 10^{-3}$ UH, which is 17.6 times larger than that

of the planar pump, 1.55×10^{-3} UH. The peak frequency ω_{max} is only slightly shifted, from $1.05/\tau$ for the planar pump to $1.02/\tau$ for the stepped pump.

Although the dimensionless variables contain all the parameter scalings and facilitate comparison between different designs, it is instructive to plug in some numbers, neglecting surface capacitance ($\delta = 0$). For typical experimental conditions[13,20] ($L = 5$ μm, $V = 1$ V) in aqueous solutions ($\lambda = 10$ nm, $D = 0.5 \times 10^{-5}$ cm^2 s^{-1}, $\varepsilon = 7 \times 10^{-5}$ g cm V^{-2} s^{-2},

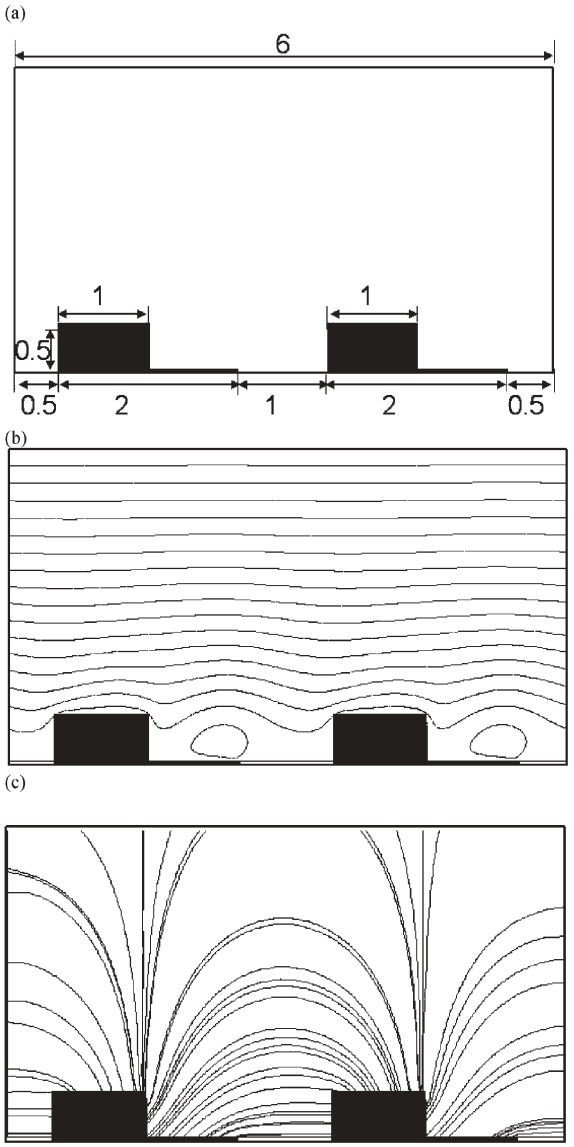

Fig. 3 Simulation of a 3D ACEO pump with a periodic array of stepped electrodes of alternating polarity in space and time. The geometry, shown in (a), has gaps and step widths all equal to minimum feature size L, so the horizontal array period is $6L$. The channel height is $20L$, far beyond the range shown above. The length L sets the scales for velocity $U = \varepsilon V^2/\eta L(1 + \delta)$ and electric field $E = V/L$. Simulation results are shown for AC frequency $\omega = 1/\tau$, near the maximum flow rate, where $\tau = \lambda L/D(1 + \delta)$ is the "RC" charging time. The time-averaged fluid streamlines (b) clearly show a fluid conveyor belt, and the electric field in phase with the voltage peaks (c) resembles the sketch of Fig. 2(b).

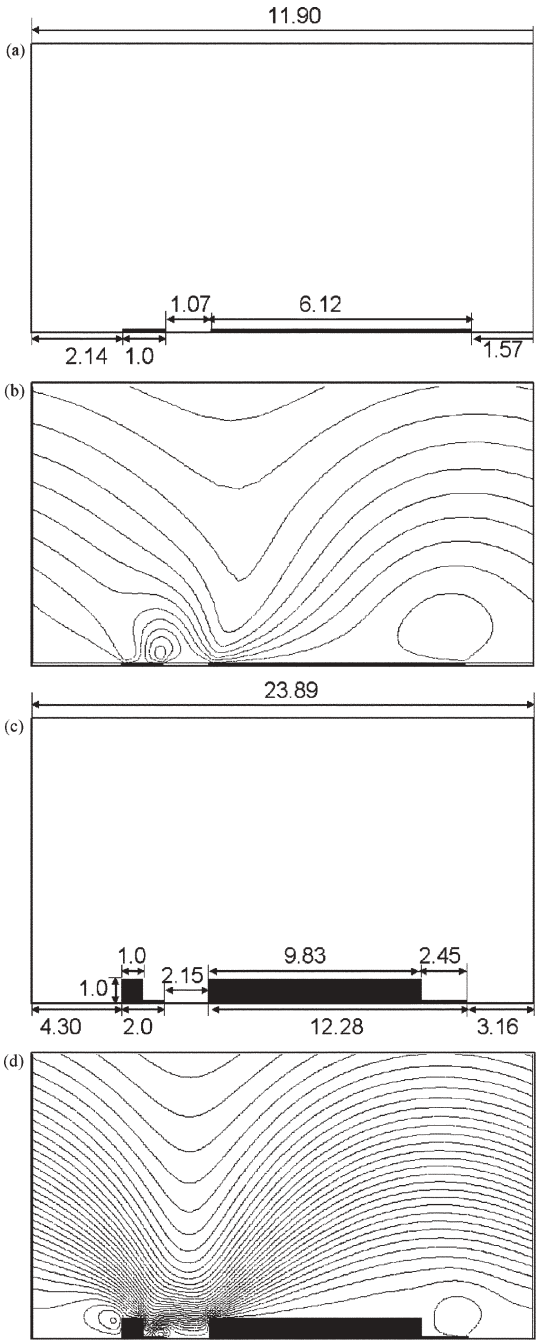

Fig. 4 The geometry (a) and simulated time-averaged streamlines (b) for the state-of-the-art planar ACEO pump proposed by Brown *et al.*[11] from the recent experiments of Studer *et al.*[13] for $\omega = 1.0/\tau$, the optimal frequency they reported. The spacings and sizes of the electrode pair are asymmetric,[11] which leads to long-range pumping from left to right, primarily driven by the larger electrode. The minimum feature size L is the width of smaller electrode, so the array period is $11.90L$. The geometry (c) and simulated flow (d) are also shown for a new design with stepped electrodes made by raising portions of the planar pump in (a) up to the stagnation points. The geometry is rescaled horizontally to set the minimum feature size L to the width of the smaller step, which results in a larger period of $23.89L$. In both simulations, the channel height is again set to $20L$.

η = 0.01 g cm^{-1} s^{-1}), the stepped pump has mean velocity u_{max} = 190 μm s^{-1} and frequency ω_{max} = 10 kHz at the maximum flow rate. The planar pump has almost the same peak frequency, but a much smaller velocity u_{max} = 11 μm s^{-1}. For a microchannel of cross sectional height H = 100 μm and width 500 μm, the stepped pump has a flow rate of 9.6 nL s^{-1}, compared to 0.54 nL s^{-1} for the planar pump. With somewhat smaller feature sizes and/or geometrical optimization, the simulations suggest that mm s^{-1} mean velocities should be attainable, while still applying only a few volts at 10–100 kHz. Such velocities are comparable to traditional pressure-driven micro-flows and scale favorably with miniaturization.

Our basic design principle is extremely robust. In Fig. 4c, we apply it to the asymmetric planar pump of Fig. 4a by raising the portion of each electrode with slip in the pumping direction by a distance equal to half the smaller gap between electrodes. For a fair comparison with the other designs, we also rescale the horizontal length so that the minimum feature size L is the width of the smaller step. As shown in Fig. 5, this design has a flow rate Q_{max} = 5.52 × 10^{-3} UH, which is four times faster than the planar asymmetric pump, although five times slower than the stepped design in Fig. 3 with a symmetric footprint (for the same minimum feature size). The asymmetric-footprint pump also has a lower peak frequency ω_{max} = 0.43/τ than the others.

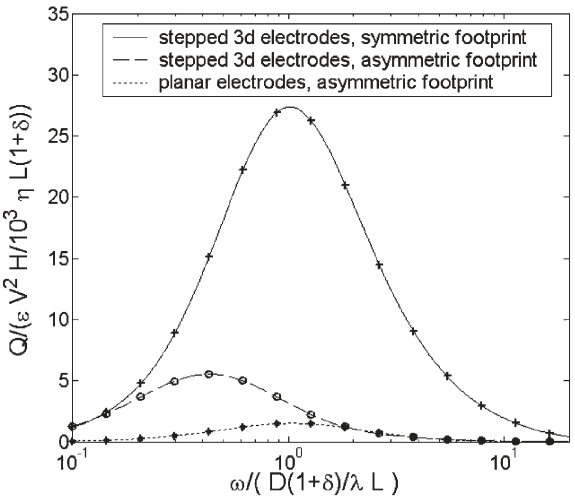

Design	Q_{max}	u_{max}	ω_{max}
stepped symmetric	27.4	1.37	1.02
stepped asymmetric	5.52	0.276	0.43
planar asymmetric	1.55	0.0775	1.05

Fig. 5 Flow rate *versus* frequency in dimensionless variables for the stepped 3D ACEO pumps in Fig. 3(a) (“stepped symmetric”) and Fig. 4(c) (“stepped asymmetric”), compared with the standard planar pump in Fig. 4(a) (“planar asymmetric”). The smooth curves are cubic splines through the simulation points. The table shows the flow rate Q_{max}, typical bulk velocity $u_{max} = Q_{max}/H$, and frequency ω_{max} of maximum pumping for each design. For typical experiments (L = 5 μm, V = 1 V, λ = 10 nm, D = 0.5 × 10^{-5} cm^2 s^{-1}), u_{max} is scaled to 140 μm s^{-1} and ω_{max} to 10 kHz. For a microchannel of height H = 100 μm and width 500 μm, Q_{max} is scaled to 7 nL s^{-1}. (These estimates neglect surface capacitance, δ = 0.)

We have found that it is not difficult to create other stepped-electrode arrays with similar flow rates and different footprints. Raising portions of any planar pump to create a fluid conveyor belt seems to always lead to a dramatic increase in flow rate, often by an order of magnitude or more. We conclude that the enhanced pumping has little to do with the layout of the two-dimensional footprint (which has been the focus of all prior work). Instead, the flow rate and frequency spectrum are much more sensitive to the geometry of the electrodes in three dimensions.

Conclusion

We have described a variety of designs for 3D ACEO pumps, which simulations predict are faster than existing planar designs by more than an order of magnitude. The crucial new concept is the ICEO “fluid conveyor belt” formed by stepped electrode arrays, where recessed counter-rotating vortices act as “rollers” for the streaming flow over the top surfaces. Simulations of a few example designs with the standard low-voltage model predict enhanced flow rates compared to a state-of-the-art planar ACEO pump[13] by almost a factor of twenty, for the same applied voltage and minimum feature size, without any systematic optimization of the geometry.

For a fixed spatial period, this enhancement seems to be rather insensitive to asymmetry in the two-dimensional “footprint” of the electrodes, which has been the focus of prior work on ACEO pumps. Instead, it seems that any footprint with appropriately raised surfaces will lead to similar, dramatic increases in flow rate, although the frequency spectrum is sensitive to the geometry. The main advantage of the symmetric footprint, aside from its simpler fabrication, is the larger minimum feature size (per spatial period) compared to asymmetric designs.

Although we have focused on pumping, our 3D stepped-electrode arrays can also be used to enhance mixing in microfluidic devices. For example, while pumping down a straight channel, mixing could be achieved at the same time with non-straight electrodes and/or raised steps having a chevron or herringbone footprint. As first pointed out for grooved surfaces in pressure-driven flows,[19] such symmetry breaking naturally leads to chaotic streamlines. Since ACEO flows have more complicated and controllable flow topology, it is likely that more efficient, self-propelled mixers can be designed.

Efforts are underway in our lab to fabricate and test the 3D designs in Fig. 3 and 4, using a microfluidic loop.[20] Preliminary experimental results indicate somewhat smaller, but still dramatic, increases in flow rate, when directly compared to planar ACEO pumps. With further simulations and experiments, we believe that more than an order of magnitude improvement in flow rate will soon be obtained in real devices.

This achievement could have a significant impact on lab-on-a-chip technology. The next generation of ACEO pumps based on these designs should deliver average pumping velocities of the order mm s^{-1} with alternating voltages of only a few volts, which could enable integration of battery power and electrical local fluidic control directly into a microfluidic chip. 3D ACEO pumps thus provide a promising platform for portable

or implantable microfluidic devices, obviating the need for complicated external plumbing (as in pressure-driven valving) or a high-voltage power supply (as in capillary electro-osmosis or flow-FET). A general limitation of ACEO is the apparent need to use low ionic strength electrolytes, due to the poorly understood suppression of ICEO flow with increasing concentration,[13] roughly above 10 mM in simple electrolytes.[21] In many systems where ACEO flows are already used,[11–13,16,22] however, manipulating biological fluids and chemical suspensions, at much greater velocities than before should not present any problems.

Acknowledgements

This research was supported by the U.S. Army through the Institute for Soldier Nanotechnologies, under Contract DAAD-19-02-0002 with the U.S. Army Research Office. The authors thank L. Olesen for valuable comments on the manuscript.

References

1 H. A. Stone and S. Kim, *AICHE J.*, 2001, **47**, 1250; D. R. Reyes, D. Iossifidis, P. A. Auroux and A. Manz, *Anal. Chem.*, 2002, **74**, 2623; D. J. Beebe, G. A. Mensing and G. M. Walker, *Annu. Rev. Biomed. Eng.*, 2002, **4**, 261.
2 M. A. Unger, H. Chou, T. Thorsen, A. Scherer and S. R. Quake, *Science*, 2000, **288**, 113.
3 G. M. Whitesides, E. Ostuni, S. Takayama, X. Jiang and D. E. Ingber, *Annu. Rev. Biomed. Eng.*, 2001, **3**, 335; G. M. Whitesides and A. D. Stroock, *Phys. Today*, 2001, **54**, 42.
4 T. M. Squires and S. R. Quake, *Rev. Mod. Phys.*, 2005, **77**, 977.
5 J. Lyklema, *Fundamentals of Interface and Colloid Science*, Academic Press, London, 1991, vol. 2.
6 C. S. Lee, W. C. Blanchard and C.-T. Wu, *Anal. Chem.*, 1990, **62**, 1550; M. A. Hayes and A. G. Ewing, *Anal. Chem.*, 1992, **64**, 512; K. Ghowsi and R. J. Gale, *J. Chromatogr.*, 1991, **559**, 95; C. T. Wu, T. Lopes and B.-C. S. Lee, *Anal. Chem.*, 1992, **64**, 88; M. A. Hayes, I. Khetarpal and A. G. Ewing, *Anal. Chem.*, 1993, **65**, 2010.
7 R. B. M. Schasfoort, S. Schlautmann, L. Hendrikse and A. Van den Berg, *Science*, 1999, **286**, 942.
8 A. Ramos, H. Morgan, N. G. Green and A. Castellanos, *J. Phys. D*, 1998, **217**, 2338; A. Ramos, H. Morgan, N. G. Green and A. Castellanos, *J. Colloid Interface Sci.*, 1999, **217**, 420; N. G. Green, A. Ramos, A. Gonzalez, H. Morgan and A. Castellanos, *Phys. Rev. E*, 2000, **61**, 4011; A. Gonzalez, A. Ramos, N. G. Green, A. Castellanos and H. Morgan, *Phys. Rev. E*, 2000, **61**, 4019; N. Green, A. Ramos, A. Gonzalez, H. Morgan and A. Castellanos, *Phys. Rev. E*, 2002, 66.
9 M. Z. Bazant, K. Thornton and A. Ajdari, *Phys. Rev. E*, 2004, **70**, 021506.
10 A. Ajdari, *Phys. Rev. E*, 2000, **61**, R45–R48.
11 A. B. D. Brown, C. G. Smith and A. R. Rennie, *Phys. Rev. E*, 2001, **63**, 016305; M. Mpholo, C. G. Smith and A. B. D. Brown, *Sens. Actuators, B*, 2003, **92**, 262; A. Ramos, A. Gonzalez, A. Castellanos, N. G. Green and H. Morgan, *Phys. Rev. E*, 2003, **67**, 056302; V. Studer, A. Pepin, Y. Chen and A. Ajdari, *Microelectron. Eng.*, 2003, **61**, 915.
12 B. P. Cahill, L. J. Heyderman, J. Gobrecht and A. Stemmer, *Phys. Rev. E*, 2004, **70**, 036305; A. Ramos, H. Morgan, N. Green, A. Gonzalez and A. Castellanos, *J. Appl. Phys.*, 2005, **97**, 084906.
13 V. Studer, A. Pepin, Y. Chen and A. Ajdari, *Analyst*, 2004, **129**, 944.
14 M. Z. Bazant and T. M. Squires, *Phys. Rev. Lett.*, 2004, **92**, 066101; T. M. Squires and M. Z. Bazant, *J. Fluid Mech.*, 2004, **509**, 217; T. M. Squires and M. Z. Bazant, *J. Fluid Mech.*, 2006, **560**, 65.
15 N. I. Gamayunov, V. A. Murtsovkin and A. S. Dukhin, *Colloid J. USSR*, 1986, **48**, 197 (english); N. I. Gamayunov, G. I. Mantrov and V. A. Murtsovkin, *Colloid J. USSR*, 1992, **54**, 20 (english): V. A. Murtsovkin, *Colloid J.*, 1996, **58**, 341.
16 J. A. Levitan, S. Devasenathipathy, V. Studer, Y. Ben, T. Thorsen, T. M. Squires and M. Z. Bazant, *Colloids Surf., A*, 2005, **267**, 122.
17 L. Olesen, H. Bruus and A. Ajdari, *Phys. Rev. E*, 2006, **73**, 056313.
18 E. Lauga and H. A. Stone, *J. Fluid. Mech.*, 2003, **489**, 55.
19 A. D. Stroock, S. K. W. Dertinger, A. Ajdari, I. Mezic, H. A. Stone and G. M. Whitesides, *Science*, 2002, **295**, 647.
20 J. P. Urbanski, J. Levitan, T. Thorsen and M. Z. Bazant, *Appl. Phys. Lett.*, in press.
21 J. A. Levitan, PhD Thesis, Massachusetts Institute of Technology, USA, 2005.
22 J. Wu, Y. Ben, D. Battigelli and H.-C. Chang, *Ind. Eng. Chem. Res.*, 2005, **44**, 2815; Z. Gagnon and H.-C. Chang, *Electrophoresis*, 2005, **26**, 3725; J. Wu, Y. Ben and H.-C. Chang, *Microfluidics Nanofluidics*, 2005, **1**, 161; J. Wu, *IEEE Trans. Nanotechnol.*, 2006, **5**, 84.